LAWRENCE
LIVERMORE
NATIONAL
LABORATORY

UCRL-JRNL-215884

Hydrodynamics of Conically-Guided Fast-Ignition Targets

S. P. Hatchett, D. Clark, M. Tabak, R. E. Turner, C. Stoeckel, R. B. Stephens, H. Shiraga, K. Tanaka

October 4, 2005

Fusion Science and Technology

Hydrodynamics of Conically-Guided Fast-Ignition Targets

S. P. Hatchett, D. Clark, M. Tabak, R. E. Turner
Lawrence Livermore National Laboratory, Livermore, California 94550

C. Stoeckl
Laboratory for Laser Energetics, University of Rochester, Rochester, New York 14623

R. B. Stephens
General Atomics, San Diego, California 92186-5608

H. Shiraga, K. Tanaka
Institute for Laser Engineering, Osaka University, Osaka, 565-0871 Japan

Abstract

The fast ignition (FI) concept requires the generation of a compact, dense, pure fuel mass accessible to an external ignition source. The current baseline FI target is a shell fitted with a re-entrant cone extending to near its center. Conventional direct or indirect drive collapses the shell near the tip of the cone and then an ultra-intense laser pulse focused to the inside cone tip generates high-energy electrons to ignite the dense fuel. Theoretical investigations of this concept with a modest 2-D calculational scheme have sparsely explored the large design space and the tradeoffs available to optimize compaction of the fuel and maintain the integrity of the cone. Experiments have generally validated the modeling while revealing additional complexities. Away from the cone, the shell collapses much as does a conventional implosion, generating a hot, low-density inner core plasma which exhausts out toward the tip of the cone. The hot, low-density inner core can impede the compaction of the cold fuel, lowering the implosion/burn efficiency and the gain, and jetting toward the cone tip can affect the cone integrity. Thicker initial fuel layers, lower velocity implosions, and drive asymmetries can lead to decreased efficiency in converting implosion kinetic energy into compression. Ignition and burn hydrodynamic studies have revealed strategies for generating additional convergence and compression in the FI context. We describe 2-D and 1-D approaches to optimizing designs for cone-guided fast-ignition.

I. Introduction and Background

Tabak *et al*[1] have reviewed the basic Fast Ignition (FI) concepts. The dense fuel core is assembled in the standard ICF way by ablative implosion[2]. Early in the development of the FI idea it became clear that some method had to be found to diminish the standoff distance between the region where ultra-intense laser light was converted to hot electrons and the dense fuel region where those electrons were to deposit their energy, since the critical surface, from which these electrons would be launched, is typically located many hundreds of microns from the core, whose size would be only a fraction of that distance. (Original ideas focused around "channeling" whereby a less intense laser would push open a channel through the ablated plasma to be immediately followed by the ignition laser pulse through the evacuated path. This idea has lacked appeal because the channeling process appears to be unstable as the channel must be pushed open up a steep density gradient.)* A target design containing a re-entrant cone was introduced to allow electron generation closer to the core[3 4] *cf* Fig. 1. A somewhat similar idea, with a less dense core, was proposed earlier[56], but was apparently unknown outside the former Soviet Union. In the west, the idea was first published by Hatchett and Tabak in a conference proceeding[7] following which it almost immediately received its first experimental test[4].

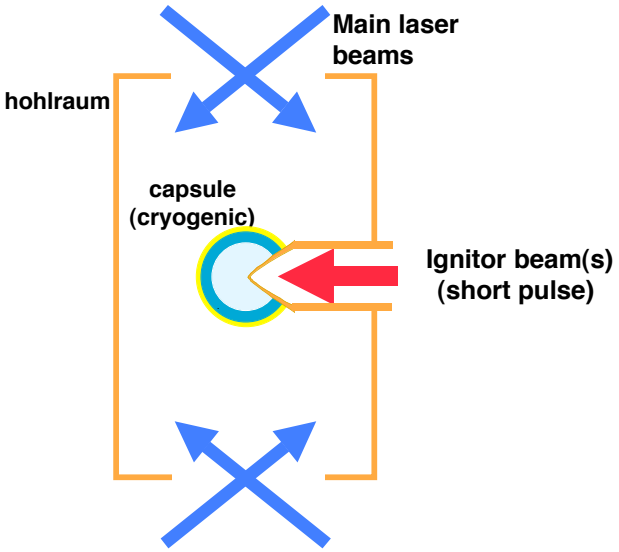

Fig. 1. Schematic for an indirectly driven, cone-guided implosion. A re-entrant tube and cone provide a vacuum path for the ignitor beam to near the imploded, high density core. The direct-drive scheme is very similar except the main laser beams shine directly on the capsule, and there is no hohlraum.

The cone was originally thought of as a device to keep open an evacuated path for the ignition laser, allowing hot electron conversion to take place close enough to the dense core that the hot electron energy would be efficiently coupled to the core even if the electrons were sprayed from their origin. Subsequent experiments and PIC simulations have appeared to show that the cone also guides and concentrates the laser beam and may concentrate the flow of hot electrons leading to remarkably large coupling efficiency[489]. Recently the concept has been incorporated into designs for ion driven fast ignition, see Key et al[10] in this volume, because the cone can

prevent x-rays from pre-heating the ion-emitting surface. Also, as we shall see, the cone, while greatly increasing the complexity of the implosion hydrodynamics, can produce the benefit for FI of "puncturing the balloon" — allowing the escape of hot, high entropy gas from the implosion center and thereby allowing a more compact core compression. The cone-guided implosion idea has been fruitful, but, unlike conventional hot-spot ignition implosion hydrodynamics, it has just begun to be explored.

Our purpose here is to review what has been discovered over the last five or so years about the hydrodynamics of cone-guided implosions for FI. In section II we will review the design goals, some of the key design parameters, our modeling tools and techniques, and baseline designs. Section III will review what experiments have shown us about the hydrodynamics — both confirming the viability of the overall scheme and our modeling methods and revealing complexities and important details. Section IV reports further design/optimization explorations in 2-D and reports some hydrodynamics insights from studies of ignition and burn in NIF-scale capsules. Within 1-D and 2-D contexts we discuss various sources of inefficiency. We conclude in section V.

II. Goals, Tools, and Baseline Design

One can start to think about the design problem as basically a 1-D spherical implosion "perturbed" by a cone poked into one side, *cf* Fig. 2. Spherical implosion is generally acknowledged as being the most efficient way to drive DT to the densities (> ~several x 10^2 g cm^{-3}) needed for inertial fusion energy or smaller scale ignition applications[2]. If the cone were idealized as a boundary condition — fixed in space with its point at capsule center, perfectly reflecting, with free slip of a fluid along its surface — then the implosion would simply be the equivalent spherical implosion but missing a sector. Most of our discussion here will be concerned with the consequences of the non-ideal behavior of real cone materials and the associated hydrodynamics. Generally one tries by design to make the cone behave as ideally as possible.

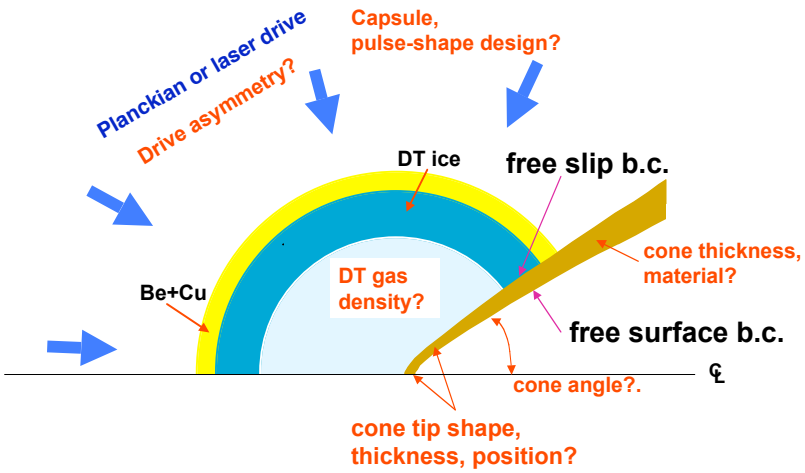

Fig. 2. 2-D Lagrangian calculation scheme and some of the design parameters to be optimized.

If the cone is to, as much as possible, remain fixed in space and reflect the momentum fluxes directed at it as the imploding capsule moves along it and stagnates near its tip, then it must be as dense as possible. (We ignore material stiffness in the context of ICF implosion pressures.) And, if the cone material is much more dense than the imploding capsule matter, one expects that for most of the implosion the capsule material will slip along the cone without entraining much cone material or generating much of a Kelvin-Helmholz instability before the imploding shell has gone by[11]. Hence the baseline design uses a gold cone.

The high x-ray opacity of gold (or other high-Z matter) will tend to make the cone reflective of the diffuse x-rays impinging on it in the x-ray drive case, but it will not be ideally reflective in the laser (direct) drive case, and one may have to design drive asymmetry to compensate for this.

If we desire that the inside surface of the cone be unperturbed until the high intensity laser is fired into it, this will dictate the minimum thickness of the cone as a function of distance from capsule center. The imploding capsule imposes a pressure impulse on the capsule side of the cone and the cone must be made thick enough that the resulting shock wave in the gold does not have time to break out on the other side where it could put gold plasma in the high-intensity laser path. Near the cone tip, however, the cone must be as thin as possible because that material will absorb energy from the hot electrons (or fast ions in the ion driven scenario) and lower the overall ignition efficiency. These conflicting requirements near the tip cannot be completely reconciled.

Near the end of the implosion, the pressures developed are such that real cone materials cannot even approximately reflect the momentum fluxes on them, and the lack of momentum from the cone portion of the capsule solid angle breaks the spherical symmetry. Less of the implosion kinetic energy can be turned into internal energy of compression, and the resulting compressed core will not be round. Grossly these effects depend on the opening angle of the cone: the narrower the angle the less solid angle is perturbed and the implosion is rounder and more efficient. However, the earliest design studies found that narrow cones were prone to being pinched shut at the nose unless they were very thick there or strongly blunted.

Making the cone as effectively thin as possible at the tip for the beam of ignition electrons means that the cone should probably be somehow blunted. How? And how far in should the cone penetrate for the "best" implosion? (Or if we think of a virtual, un-blunted cone, where should the point be relative to capsule center? For compression efficiency? For putting the compressed core closer to the cone?)

We may use asymmetric drive to compensate partially for the asymmetry due to the cone, and/or we may use it to improve the final state in some other way, say to put the compressed core closer to the cone tip.

Then, there is the whole new design space for optimizing the 1-D implosion discussed by Tabak in this volume[1], and about which we shall say more in section IV.

Most of the design studies reported to date have been done with the LASNEX radiative-hydrodynamics code[12]. The 1-D calculations are straightforward enough. To make progress on the 2-D problem in the face of the extreme shear between the imploding capsule and the cone we

have used the scheme shown in Fig 2. The free slip boundary condition between the capsule and cone materials greatly simplifies the physics in the calculation: The two materials are coupled only by radiation flow between them and normal pressure across their mutual boundary. Remarkably, this simple scheme has proven reliable, *vis a vis* experiments (section III) and test calculations with a much more compute-intensive scheme without the free slip condition but with modern ALE methods[13].

Clearly there is an enormous design space to be explored, and only a few forays have been made. Most of the baseline design studies have been made at "NIF scale" wherein the capsule absorbs about 100-200 kJ, and then those designs have been scaled down or up, as appropriate for Gekko or Omega experiments, for planned sub-ignition experiments on Omega-EP or NIF, or for inertial fusion energy (IFE). After some computational experimentation with the cone parameters described above and with the 1-D capsule design, we arrived at the NIF-scale baseline design shown in Figure 3.

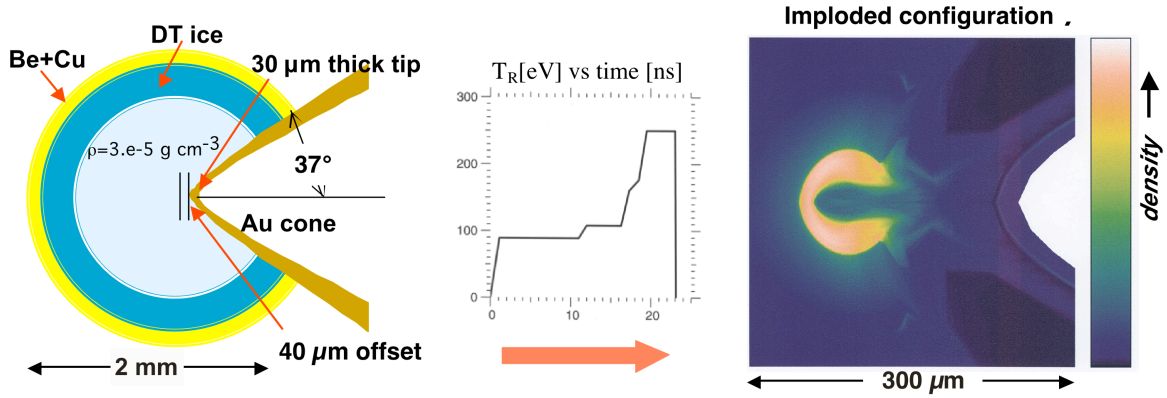

Fig.3. Baseline design for indirectly driven, NIF scale, cone-guided FI target. The capsule absorbs about 150 kJ of x-rays and the imploded configuration has a solid-angle-averaged fuel column density, $\langle \rho R \rangle_{DT} = 2.18$ g cm^{-2}.

The capsule is basically a standard NIF design[14] modified to have a thicker fuel layer, therefore imploding more slowly to a thicker, less dense shell. The initial central gas density corresponds to the vapor pressure of DT at about 15 °K. The cone tip was blunted by making the surface a hyperboloid, and the 40 μm offset was determined from a scan of that parameter.

The collapsed configuration shows several pleasant features - near spherical symmetry, a satisfactory $\langle \rho R \rangle = 2.2$ g cm^{-2}, and a nearly unperturbed cone interior. However, the collapsed configuration is not ideal. Instead of the ideal solid blob described by Tabak[1], we have a core with a hollow center. Also the blob is more than a full blob diameter from the surface where hot electrons would be generated. Finally, there is no dense fuel to ignite directly in front of the cone — ignition would have to take place off center or in an extended ring. Nevertheless these results were sufficiently promising that several experimental campaigns have been undertaken to see if Nature agrees with our calculations.

III. Experimental Tests

Within a few months of the first publication of design calculations made along the above lines[7], Kodama *et al*[4] tested the cone-guided implosion hydrodynamics on the Gekko XIII laser at the University of Osaka using a CD shell on a gold cone. A self-emission x-radiograph showed "a well imploded core plasma on the tip of the cone". From backlit radiographs (unpublished) those authors indirectly inferred that the implosion created a central core of density ~50-70 g cm^{-3} and 40-45 μm diameter — performance only marginally below that of a full spherical implosion, as driven by the 12 Gekko beams.

Since then, x-radiographs (backlit and self-emission) of indirect and direct-drive cone guided implosions at Omega and direct-drive implosions at Gekko have provided direct evidence that the implosion hydrodynamics is indeed approximated by calculations as above; the experiments have revealed some important details; and they have begun to suggest improvements.

Stephens *et al*[15] have reviewed most of the important results, some of which we shall recapitulate here:

1. Cone-guiding works — cones like those used in the experiments do not destroy the implosion to a dense core.
2. At Omega scale, pre-heat of the cone tip, especially for indirect drive, leads to some gold mixing across the cone-core gap. (This effect is not captured by the modeling scheme described, but it also does not scale to NIF or IFE implosions.)
3. A jet from the implosion core center does impact the cone tip.
4. Mis-alignment of the cone axis to capsule center and/or drive asymmetry can lead to degraded core density and possibly turbulent mixing of cone material into the cone-core gap. (2-D codes cannot capture this effect.)
5. As far as it can go, the calculational method described above is a useful design tool. The implosion and jet impact effects are reasonably well modeled.

The cryo-ignition target in Fig. 2 was re-sized to Omega[16] drive energy, first for x-ray drive[17] and then for direct laser drive[18], to test the model predictions. X-ray drive targets [Fig. 4(a)] were driven exactly as a 1/2 mm diameter conventional hot-spot (CHS) shell in a scale-1 hohlraum using 14 kJ of drive power. The re-entrant cone (dimensions as in the model: Opening angle 70°, the tip 40 μm from the center of the shell) was notched outside the shell to prevent an excessive x-ray flux on the cone near the shell. The direct-drive targets had a ~ 1 mm diameter shell [Fig. 4(b)]. The cone base blocked one set of beams entirely. The shell was driven with 11 kJ from 15 half-power and 20 full-power beams (for optimum drive symmetry, most of the other beams being used for backlighting). In the cases illustrated here the targets were backlit with He-like Fe or V Kα radiation (6.7 and 5.0 keV respectively) from a film hit with delayed beams (8 beams delayed 1.4 ns on the outside of a 7 μm foil for x-ray drive and 15 beams, delayed 1.8 ns on both sides of a 10 μm foil for direct). The sensitivity of the framing camera was determined by reference to a calibrated time integrating x-ray spectrometer[19]. The emitted spectrum,

convolved with the camera filter transmission and the spectral sensitivity of the camera[20], was compared to the backlighter intensity, integrated over backlighter area (a vertical and horizontal super-Gaussian fit was used to account for the part of the backlighter hidden behind the target) and summed over the camera frames. An identical framing camera on the other side of the chamber observed the self-emission of the target without any backlighter.

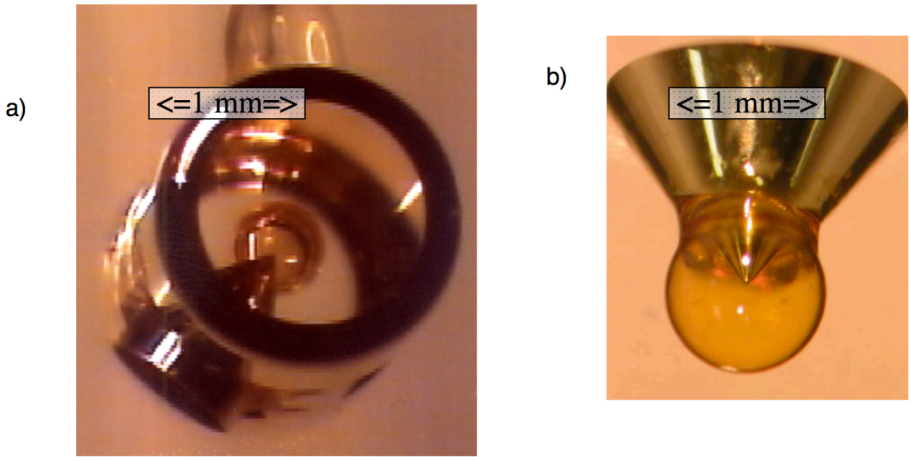

Fig. 4. X-ray drive (a) and direct laser drive (b) targets used to test the hydrodynamics of cone-guided implosions on Omega. Dimensions are shown by the 1mm scale.

The tests were made with nominally symmetric targets and symmetric drives, so we expected a collapsed geometry as in Fig. 3. A collapsed x-ray drive target is shown in Fig. 5 and a direct drive target in Fig. 6. Targets were either empty or filled with 5-10 atm of D_2 or D^3He. In all cases the cone tip [initially blunt, hyperboloidal *cf* Fig. 4(b)] appears distorted. For the x-ray drive case (Fig. 5) opacity extends between the shell and the cone. For direct drive (Fig. 6) there is a clear separation, but since the interstitial area is brighter than the backlighter, that intensity must include some self-emission, which could be masking absorption. Gas-filled, direct-drive targets showed obvious self-emission near stagnation. Detailed investigation of these images revealed a number of shell-cone interactions occurring in fast ignition targets that must be taken into account in their design.

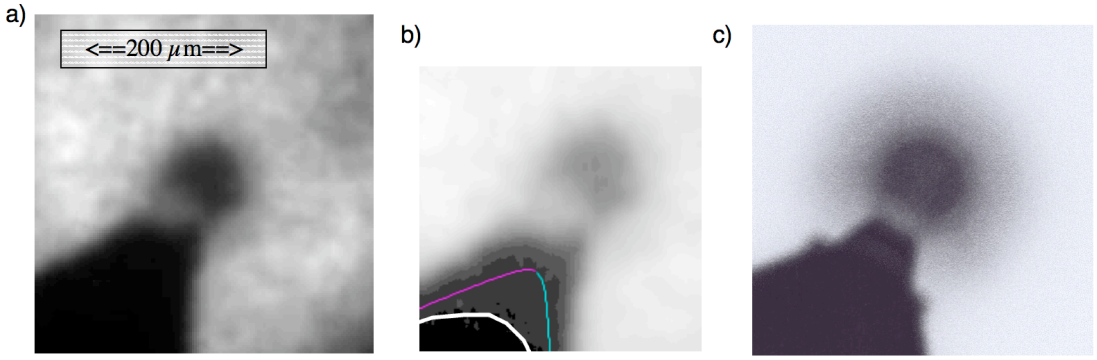

Fig. 5. Back-lit x-radiograph images of x-ray drive targets at stagnation with a) linear and b) log gray scale, and c) simulation using linear gray scale. The experiment, unlike the simulation, shows a thread of opaque material leaking from the cone into a dense shell center. In b) the thin colored line shows the original shape of the cone, the thick white line shows the border of the completely opaque region. All the images are to the same scale.

Cone Heating/Au Contamination

The fuzziness of the cone outlines in the back-lit images (especially in x-ray drive, Fig. 5) is caused by a surrounding cloud of Au vapor, ablated from the cone tip by hard x-rays. In the x-ray drive case, these are non-thermal Au M-lines in the emission from the Au hohlraum (~6% of the total incident energy for our targets[21]), and in the direct drive case they are bremsstrahlung from the laser heated CH shell. In an Omega-scale CHS target these weakly absorbed spectral components cause a mild preheating of the imploding shell. In a re-entrant cone FI target, such penetrating radiation (~1.5-4.5 keV with peak at 2-2.5 keV) is absorbed by the surface of the cone. LASNEX calculations suggest that the energy incident on the cone at this scale is ~40 kJ cm^{-2} in the x-ray drive case and ~ 9 kJ cm^{-2} for direct drive. In neither case, at this scale, is that flux easily eliminated. For x-ray drive, all of the useful high-Z hohlraum materials emit non-thermal lines in the same energy band. For direct drive the bremsstrahlung induced by the laser-generated-hot-electrons scales with Z^2 of the shell material; it would be reduced somewhat with a $BeCu_x$ shell and considerably more using a DT wetted, cryo-foam target (which reduces the C density by nearly an order of magnitude).

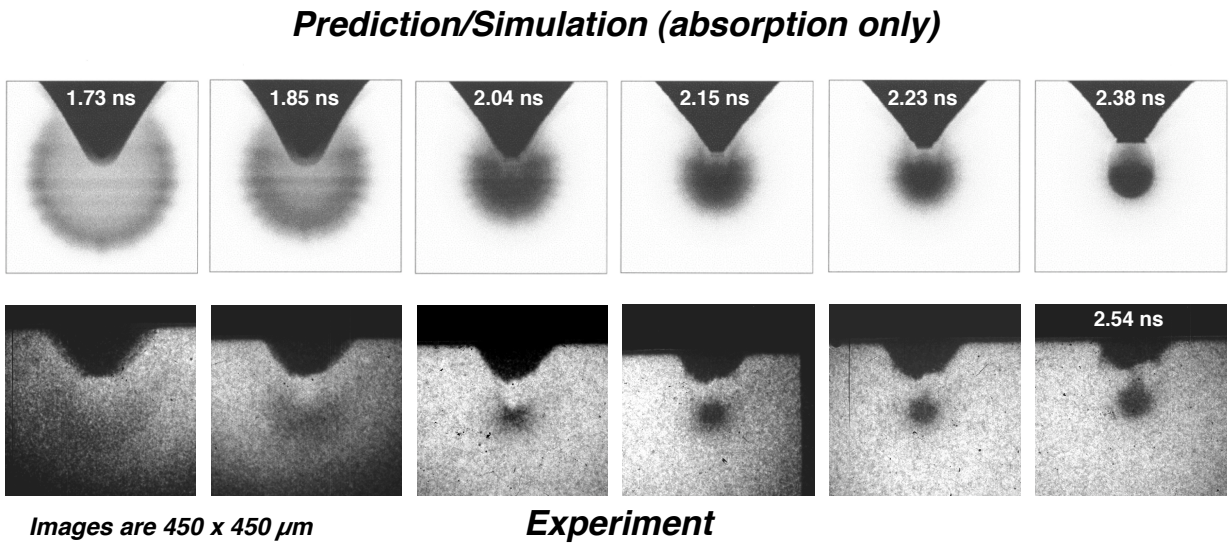

Fig. 6. Simulated and experimental backlit x-radiographs of directly-driven Omega targets. These experimental radiographs (using a Vanadium, ~5 keV backlighter) show a strong cone-shell interaction at late times, and perhaps more convergence than predicted.

This incident energy, absorbed in <1μm of the Au, generates a dense vapor layer (~0.5 g cm^{-3} - clearly seen in the first images of Fig. 6) that is at times Rayleigh-Taylor unstable[11] against the jet of lower density gas escaping the collapsing shell (discussed further below), so mixing is expected. The calculation method desribed above would not ordinarily have the resolution to capture this physics, and at any rate is not 3-D. In the x-ray drive case a filament of Au vapor can be seen to cross into the dense implosion core [Fig. 5(b)]. The contamination is apparently much more limited in the direct-drive experiments, but its extent cannot be measured with opacity, as in indirect drive, because of self-emission from the hot core. This self-emission is as bright as the backlighter in some cases and gives the illusion of a complete separation between cone and collapsed shell [as in Fig. 7(a)] unless a whole sequence is examined (Fig. 6).

Within the collapsing shell, LASNEX simulations qualitatively replicate the time evolution and shape of the self-emission as well as the evolving shape of the target, but overestimate the absolute value of both self-emission and opacity. The maximum self-emission intensity varies at least a factor of 2 from shot to shot. Since the framing camera only detects $h\nu > 2$ keV >> kT, the measured intensity is extremely sensitive to the gas temperature. A reasonable assumption is that mixing, varying with laser drive, target surface, and axial symmetry deviations [Fig. 7(b,c)], is the cause of both the low self-emission intensity and its variability.

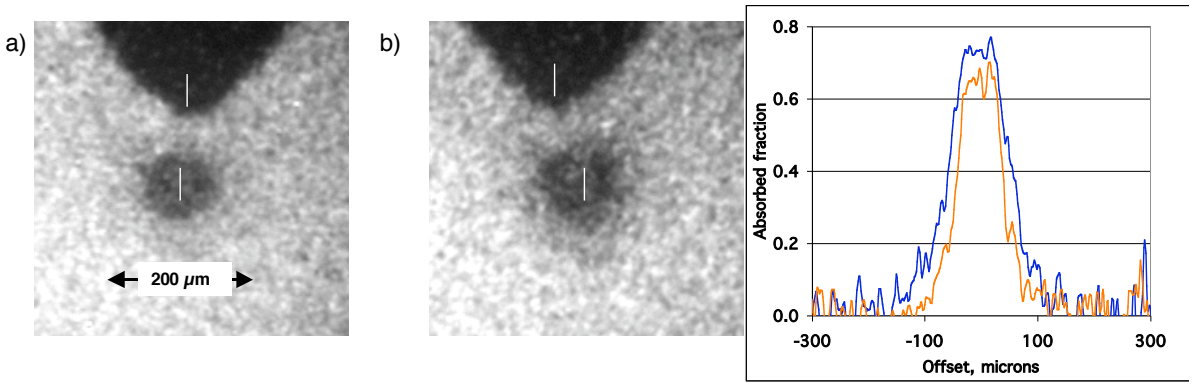

Fig. 7. Back-lit x-radiograph images of direct drive targets at stagnation a) with Fe filter to (largely) eliminate self-emission, and b) with same filter and off-center collapse. Each contained ~ 5 atm D_2. Cone and core centerlines are drawn as guides to show the ~25 μm offset in b). c) Lineouts across the images in a) (red) and b) (blue) showing that the offset limited the compression (FWHM increased from 80 to 120 μm), and reduced core gas self-emission (the apparent absorbed fraction increased from 0.65 to 0.75).

The brightness analysis of the images by Stephens *et al*[15] clearly demonstrates that any Au that might be contaminating the dense core is greatly reduced by direct as opposed to x-ray drive. We note here that at NIF or IFE scale, this effect is expected to be insignificant. The x-ray fluence on the cone tip is exponentially attenuated by the increased opacity of the much thicker ablators.

Shell-Cone Axial Alignment

For FI of the dense core to work we require that the shell collapse to a pre-determined point in front of the cone tip. Experiments showed that a cone offset from axial alignment with shell center of more than ±10 _m (at Omega scale) causes a) turbulent mixing of the core with the wall and b) prevents an optimum collapse [Fig. 7(b,c)]. Such an offset can be caused by asymmetric drive, or shell mis-placement or mis-orientation in the target chamber. It appears, in the Fig 7 case, that the cone axis was tilted ~ 5° from nominal, shifting the center of collapse and limiting the compression. This is a 3-D effect not captured by the calculation method above.

Jet/Cone Collapse

Whether or not the shell is initially filled with DT vapor or other gas, there will be some lower density plasma in a central hollow before the implosion stagnates to high shell density. The implosion drive launches two to several shocks that break out of the inner shell surface, and the rarefactions into the central cavity following shock breakout put low density plasma there that is not completely swept up again by the inward accelerating shell. When this gas stagnates at the center and is then compressed by the shell, it is at much higher entropy than the shell so it remains at lower density than the shell in the isobaric condition that obtains then. If there is vapor or other gas initially present, it is already at higher entropy than the shell and the shocks breaking out into it generate higher entropy yet, and this, of course, is how the desired CHS is formed in conventional inertial fusion implosions. One of the key points of a conventional spherical implosion is that this gas has no place to go so must get compressed and hot, but the spherical symmetry is broken by a cone in the case we consider here. The shell near the cone

sees less drive than it does elsewhere: less "sky" in the x-ray drive case, and no oblique laser rays from the cone side in the direct-drive case. Hence the shell implosion there will tend to lag slightly the rest of the implosion. Near stagnation this results in a pressure gradient between the core center and the low density gas inside the shell but over next to the cone. This drives a jet of plasma from the core center toward and past the cone tip. We will say more about this important effect in the next section; it shows up clearly in the Omega experiments.

The cone seen in indirect drive experiments (the opaque region in Fig. 5) appears considerably blunted compared to its original shape. That is expected; the central gas is flowing directly toward the tip, eventually punching it in, as seen in Fig. 7. At this time simulations show a gas jet with density ~10-20 g cm^{-3}, heated to ~400 eV, and moving at ~10^7 cm s^{-1}, for an initially empty shell. The density is doubled and the velocity ~ halved for filled shells. In simulations. the cone tip collapse starts later for a filled, compared to empty, shell. Since it is through that tip that the ignition energy is transmitted, the timing of its collapse is of vital interest. The simulated backlit images show, qualitatively through the position of the Au vapor, that the boundary is not pushed down against the tip until just before stagnation. Experimentally, that layer vanishes somewhat earlier (Fig. 6 simulation image 3 and experimental image 2). The tip collapse was investigated quantitatively using the shadow of a ledge partway down the cone as a stable reference point [Fig. 9(a)]. Fitting all the images in each shot to a 3-D model allowed determination of the fixed parameters in a sequence (cone axis tilt and ledge radius), and the height of each cone tip above its ledge as a function of time [Fig. 9(b)]. The measured collapse rate agrees quite well with that predicted by simulation. Both indicate that the tip (initially ~50 μm thick) collapses by 20-30 μm before stagnation — about the cone tip thickness one would use in an ignition target — so the tip could be penetrated before the shell mass is assembled and the ignition pulse can be delivered.

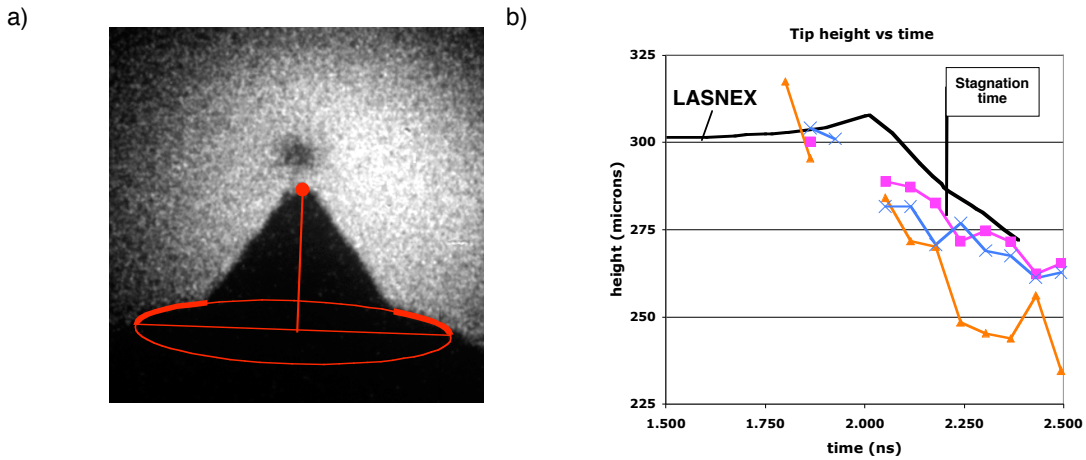

Fig. 8. a) The actual tip height was calculated by fitting the shadow of the ledge to an ellipse whose orientation and size was held fixed for all images in a sequence and assumed to be centered under the tip. b) Calculated tip height vs time for filled(triangles) and capsules (squares and Xs), and from LASNEX simulation of a gas filled capsule (smooth line). The LASNEX curve shows the "observed" tip collapse. The simulation shows the initial collapse starting ~ 0.2 ns earlier but being hidden from view by the region around it (as in Fig. 5b).

Ultra-fast self-emission x-radiographs (> ~2 keV) of the Omega implosions made with the Multi-Imaging X-ray Streak Camera (MIXS)[22] show in exquisite detail the emission from the jet/cone impact coming first and then the core assembly emission. The MIXS pictures and the backlit images nicely complement each other to give a vivid visual impression of what the implosion, jet, and cone look like, where the emission comes from, and how things evolve with time: Fig. 9.

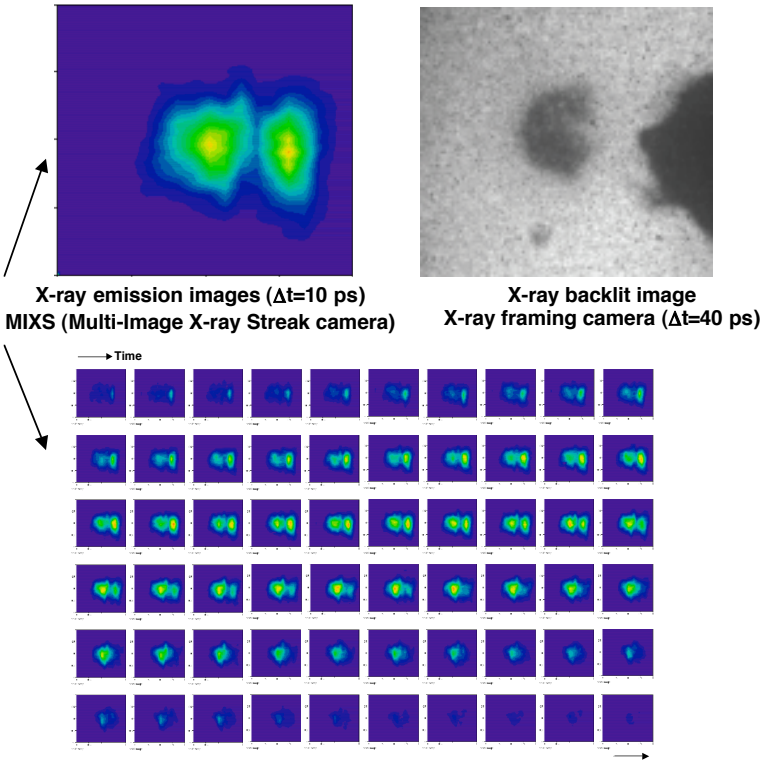

Fig. 9. MIXS self-emission images complement the backlit Omega capsule implosion images. The time sequence clearly shows emission from the jet impacting the cone and then emission from core stagnation.

Imploded Core Density

The maximum column density through the core, ρR_{max}, was determined experimentally from backlighter absorption and with proton energy loss spectroscopy[1718]. For that determination the backlit images used an Fe backlight ($h\nu$~6.7 keV) and filter to discriminate against self-emission. Absorption was determined from lineouts perpendicular to the cone axis and from comparison with a fit to the non-uniform backlighter intensity. The results were fitted to a uniformly dense solid sphere model. X-ray drive targets appeared significantly more dense than direct-laser drive targets, ~100 mg cm^{-2}, possibly the result of mixed-in Au. The column density of D^3He-filled direct-drive targets could also be evaluated using proton energy loss spectroscopy. Detectors placed on a line-of-sight away from the cone gave column densities ~ 60 mg cm^{-2}, similar to those from the absorption measurements, ~80 mg cm^{-2}.

Comparison between ρR_{max} obtained and calculated gives a measure of success in achieving clean compression. For CHS shells, the standard of comparison is a 1-D calculation. On that

basis these shells achieve ≥50% of 1-D; a respectable number. A 2-D LASNEX calculation shows that, in a re-entrant cone target, a substantial part of the core gas can escape (see discussion above) allowing the shell to collapse further. So experimentally these FI targets should perform better than CHS shells on this measure.

IV. Design Issues and Target Optimization

2-D Variations on Baseline Design

The baseline design implosion described in section II (Fig. 3) and the sorts of implosions seen in the experiments, while promising, are certainly not ideal for FI. The open ended, hollow core seen in the baseline design means a) some energy has been lost compressing and/or jetting the low density central gas, and b) this configuration will be more difficult to ignite as there is no dense material to ignite, *ie* with $\langle\rho R\rangle \sim 0.5$ g cm^{-2}, [1] directly in front of and close to the cone tip. Hence, either a ring of dense material must be ignited or an off-axis igniter beam must be used. Also, the cores are not as close to the cone tip as one would like — leading to a loss of ignition efficiency if the igniter beam spreads beyond the angle subtended by the dense portion of the core to be ignited. Finally, the cone necessarily implies lack of momentum balance at stagnation so that less kinetic energy stored up during the implosion can be converted to compression.

A narrower cone should lead to better momentum balance and a smaller residual kinetic energy fraction in the fuel. Fig. 10b shows a calculational test of this idea. The collapsed configuration of the core is improved, but the combination of transverse pressure on the cone from the imploding shell, and then from the central jet as it splits around the cone, pinches the cone tip. This has a sort of scissors effect closing down the cone interior and potentially putting the origin of the igniter beam 30% further away, implying 40% less igniter intensity on the dense core for a divergent beam. Perhaps this scissors effect can be mitigated by changing the cone tip shape. Integrated experiments with both 60° and 30° (full angle), flat tipped cones at ILE Osaka have shown good energy coupling (20%) between the short pulse laser shot into the cone and the imploded blob.[23]

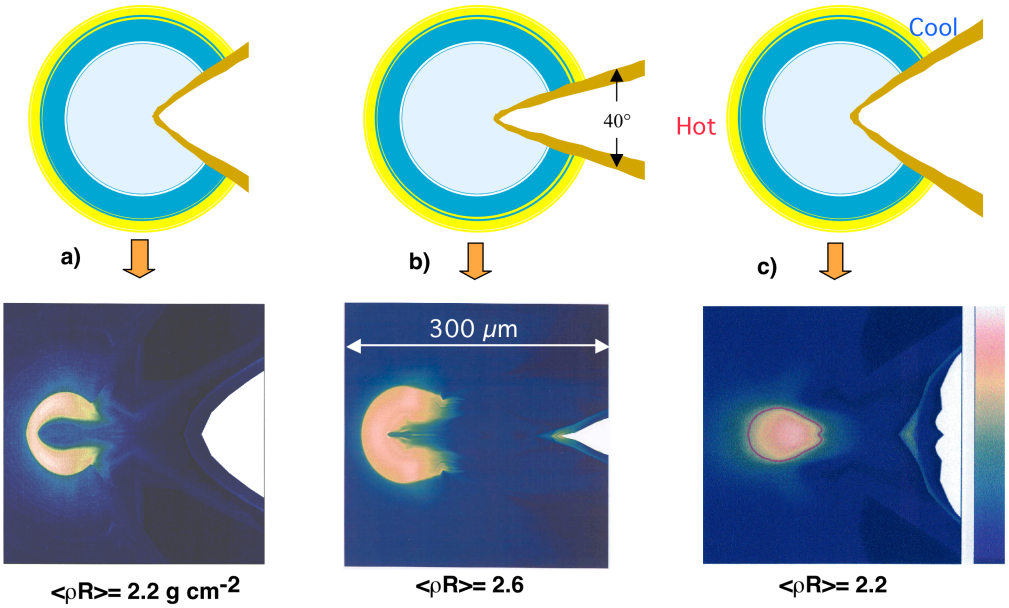

Fig. 10. Variations on the NIF-scale baseline design a). Narrower cone, b) produces a less hollow core and higher <ρR>, but jet pinches cone so that cone vacuum is 30% further away. Asymmetric drive, c), which has 10% P_1 in flux, in the sense shown, produces a very compact core that is closer to cone vacuum, but the jet has strongly impacted the cone tip, and the red density contour contains only about 10% of the original fuel mass.

We have also done calculational experiments on the baseline design to look at the effects of drive and capsule asymmetries in moving the core closer to the cone and/or producing a more compact core. Fig. 10c, showing an apparently successful result was an implosion with a 10% P_1 drive asymmetry. The core is much more compact as the central plasma is pushed completely out toward the cone. However, the momentum imbalance is more severe, and the enhanced impact of the jet on the cone is obvious.

When we conducted studies of the *ignition* of the NIF-scale capsules (which is not the main focus of this paper), we did uncover some interesting hydrodynamics which we discuss below.

Ignition of the asymmetrically driven capsule, Fig. 10c, showed an implosion efficiency problem[*]. The core could be ignited by a collimated, 60 μm diameter (roughly the size of the dense core), beam of 20 MeV protons, with total beam energy of 35 kJ. (Alternatively it could be ignited by a 40 μm diameter, collimated beam of 1.6 MeV electrons of total energy 30 kJ). In either case the igniting particles were stopped near the perimeter of the dense core if they flew straight, which was a simplifying assumption for this study. The yield was 30 MJ (or 27 MJ for electron ignition), representing a burnup fraction of about 13% of the total DT fuel. Since the implosion cost about 150 kJ absorbed into the ablator, or about 10 times that in laser energy, for the NIF scale hohlraum, the gain does not seem very impressive on any assumption about the conversion of ultra-intense laser energy into an igniting particle beam. But, the dense, egg-shaped core in Fig. 10c contains only about *10%* of the fuel mass (inside red contour), and in

[*] In retrospect, your first author should have noticed this earlier, but then the physics of the remarkably high burn efficiency found for this configuration might have been missed!

this material about *50% of the energy is still kinetic*. Overall, about 60% of the fuel energy at this time is still kinetic. So this asymmetric drive strategy has produced a compact blob at a rather high energy cost per blob mass, in part because the momentum imbalance does not allow a large fraction of the implosion kinetic energy to be converted to internal energy of compression at stagnation. Table I compares the implosion energetics for the baseline capsule, Fig. 10a, the narrow cone capsule, Fig. 10b, and the asymmetrically driven capsule, Fig. 10c.

	Baseline Capsule	Narrow Cone	Asym. Drive
$\langle\rho R\rangle_{fuel}$ [g cm^{-2}]	2.15	2.60	2.20
mass fraction in blob [%]	36-40	40-44	9-13
fuel total energy [kJ]	13.0	14.1	14.1
fuel kinetic energy [kJ]	4.1	3.8	8.3

Table I. A comparison of some implosion figures-of-merit for the NIF-scale capsule implosions shown in Fig. 10.

We note here that the main fuel in CHS capsules typically implodes as a high aspect ratio (R/ΔR) shell and can stagnate nearly all at once to peak <ρR>. The thicker fuel layer in a capsule such as the baseline design here implodes with a lower aspect ratio, and unless the implosion drive can be tailored to produce a rather special radial profile of density and velocity (see below), then max <ρR> will be created by an inner fraction of the fuel while the outer fuel is still imploding. Subsequently that inner fraction will be expanding even while the outer fuel is stagnating onto it, with total <ρR> *de*creasing. Furthermore, there is always some residual kinetic energy in these thick fuel capsules at peak <ρR> even if the implosion is essentially 1-D.

Burn Efficiency

On the other hand, the burn efficiency of the asymmetrically driven capsule was found to be remarkably *high*. The baseline capsule, when ignited by a broad (axially symmetric) beam gave a yield of about 30 MJ, which is about the same as that of the asymmetrically driven capsule in spite of having about 3 times as much fuel in the dense blob! The reader may have noticed that the 30 MJ yield reported above for the asymmetrically driven capsule, while representing burn-up of ~13% of the total fuel, represents something like *100% burn-up* of its dense blob. Figure 11 shows some of the physics of its ignition.

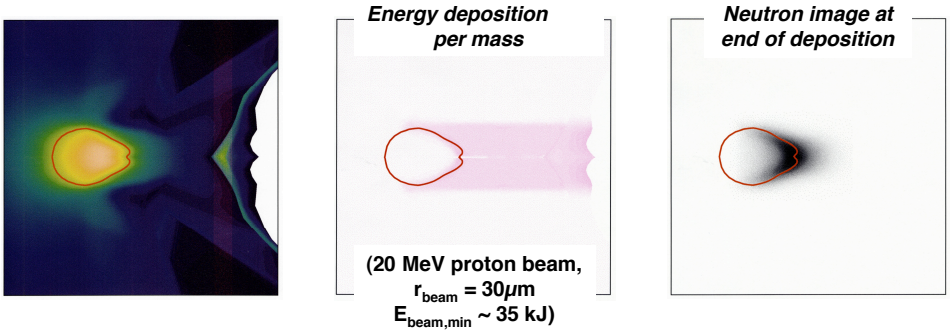

Fig. 11. The *shape* of dense core and of the ignitor deposition can generate additional convergence which generates a very robust ignition and a higher fuel <ρR> for higher burn-up fraction and higher yield.

When this capsule was ignited, the beam energy, because of the very steep density gradient, was absorbed in a sort of "cap" on and around the end of the egg-shaped core. This is shown by a simulated neutron image at the end of deposition showing where burn is initiated. Pressure developed by burn in this region strongly drove additional convergence of the remaining dense fuel, increasing its <ρR> and driving axial material to rapid burning. Herrmann et al[24] reported this physics as a means of decreasing the fast igniter beam energy by using a ring shaped beam to heat a ring rather than a spot on a solid, dense DT blob. This effect was not seen in the burn of the more spherical baseline capsule with its hollow center. Hermann et al noted that an igniting hot spot prepared by heating a portion of a dense blob of fuel (which is the fast ignition scenario of so-called isochoric heating) requires substantially more energy into the hot spot than the isobaric heating of the hot spot in CHS ignition. Isochoric ignition produces far larger pressure gradients, and the high pressure region is at the edge of the fuel. Hence the hot spot can fall apart more rapidly. The above convergence effect can help mitigate this. We believe this burn-driven, additional compression effect should be studied further in the Fast Ignition context where ignition near the surface of the fuel can exploit the effect.

We also noted in our studies of the ignition of cone-guided implosion cores, that it was very difficult to achieve significant burn up fractions from cores with <ρR> <~1.5 g cm^{-2} no matter how robustly they were ignited. To our knowledge, the physics behind that threshold is not well understood, at least in the way that the formula, $\phi = \rho R/(\rho R + 6g\,cm^{-2})$ where ϕ is the burn up fraction, is understood for CHS ignition[25]. Certainly, for ignition, one should design cone-guided implosions to achieve <ρR> > 2 g cm^{-2}.

Cones with holes

We have remarked above that a hot, lower density center to the dense core (*cf* Fig 10a,b) is a robust, non-ideal feature. Drive asymmetry can eject it, but at an efficiency cost. If not ejected, then the core is not ideally compact for ignition, and some implosion kinetic energy must be spent compressing it (~10% in the baseline capsule). For some ignition schemes, *e.g.* proton fast ignition[10], a small amount of plasma in the cone interior may be preferable to a dense, distorted cone tip which can absorb and disperse beam energy before it can reach the fuel. We have investigated whether the central hot plasma can be ejected as a jet through an opening in the

cone tip. In this case, our simulations compared directly-driven, *Omega-scale* implosions, with an eye toward near-term experimental tests.

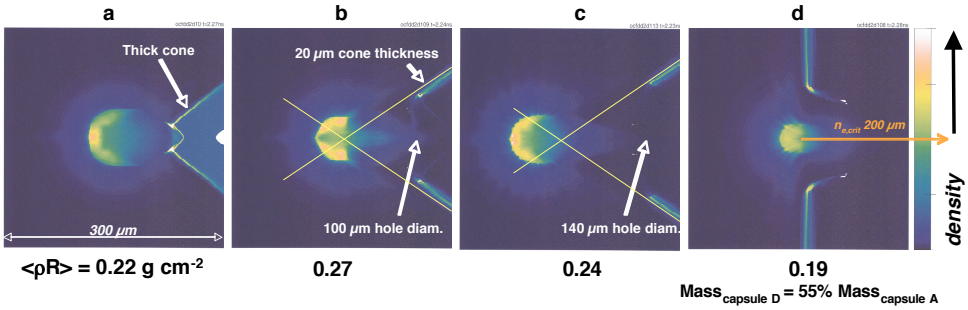

Fig. 12. Omega-scale direct drive implosion simulations showing peak <ρR> configurations to demonstrate the effects of implosions along cones with gaps at the cone tip. Simulation D shows the result for a hemi-spherical capsule (180° "cone"). In all three simulations with holes the plasma jet from the capsule put the critical density for 1μm laser light at about 200μm from the dense core.

Fig. 12 compares four implosion simulations with capsules and drive as used in the Omega direct-drive experiments described above. The initial gas fill in the capsules, and inside the cones with holes was 1.e-5 g cm^{-3} of CH, so they were effectively nearly empty. There was a free-slip boundary condition on both sides of the cones with holes. Fig. 12a shows an implosion along an extra thick cone (effectively solid) so that the effects of cone distortion are minimized. Fig. 12b shows the collapse for a 20 μm thick cone with a 100 μm diameter hole at its tip. This clearly shows an improved core configuration - more compact and higher <ρR>. Fig. 12c shows the result of opening the cone further to twice the hole area and moving the cone's (virtual) tip outwards 30 μm to partly compensate the wider hole by putting it further from capsule center. The result is intermediate. Finally, in Fig 12d we look at the result of opening the "cone" up to 180°, a flat plate. This result is also promising: The <ρR> is more than 2/3 the value for the 12b capsule in spite of the asymmetry and having only 55% the capsule mass. This last 180° "cone"-with-hole geometry has begun to be investigated extensively in the context of fast ignition on the Z-machine at Sandia National Lab., Albuquerque[26]. Backlit radiographs of such implosions have been reported as having been made[27], but are apparently unpublished as yet. Calculations, such as those shown here, predict the plasma configuration within the cone as well as the x-ray flux through the hole. Those predictions must be studied further to investigate the potential effects of the plasma on laser-beam propagation, hot electron generation and transport, proton beam transport, and the effects of x-rays on a proton beam emitting surface[10].

1-D Optimization

We have remarked above on two essentially 1-D design issues: the central hot plasma that inhibits burn efficiency and must be compressed unless jetted away to the detriment of the cone; and the thick fuel layer which does not stagnate all at once, leading to unutilized implosion kinetic energy. Below we take up these issues in turn.

Several solutions have been proposed for the central gas problem including enhanced mix to lower its entropy, high-Z dopants to radiate its entropy away, and other cones with holes to jet it

away (away from the igniter beam cone). We have investigated all but the last of these, but the simplest fix appears to be initially colder fuel and a careful pulse shape. Initially colder fuel has a lower vapor density filling the capsule, and careful, tight pulse-shaping can minimize the amount of plasma blown into the interior by shock breakout. Fig. 13 compares the final density profiles (at peak <ρR>) for the NIF-scale baseline capsule (in a 1-D simulation) and for one with 1/30 the initial vapor density (T=11.5 °K vs 15°K)[28]. Final <ρR> is increased by 10% and the central cavity is somewhat smaller.

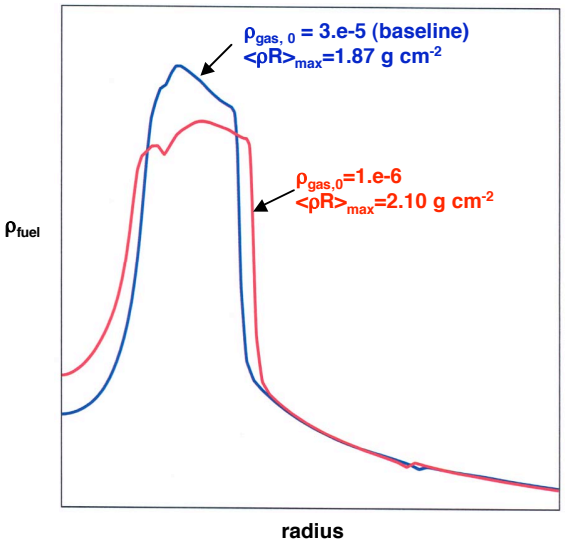

Fig. 13. Density profiles at peak <ρR> for the baseline, NIF-scale capsule with an initial DT vapor density in the capsule of 3.e-5 g cm^{-3} (blue) and for the same capsule with an initial vapor density of 1.e-6 g cm^{-3} (red). The initial vapor densities correspond to initial cryogenic DT temperatures of about 15°K and 11.5°K respectively.

Figs. 14 and 15 illustrate a graphical method for looking at the central plasma and thick fuel problems.

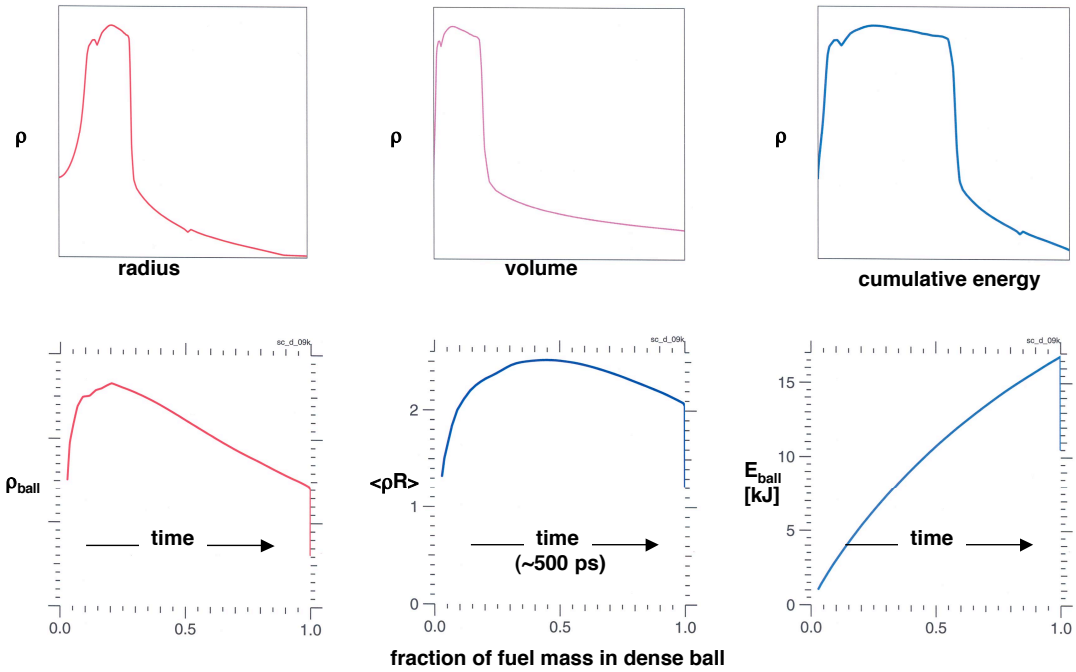

Fig. 14. Central gas and thick fuel effects in a 1-D simulation of the implosion of the NIF-scale baseline capsule with initial vapor density of 1.e-6 g cm^{-3}. The top three plots are "snapshots" at peak <ρR> of the runs of density *vs* radius, *vs* cumulative volume (r^3), and *vs* cumulative energy. The bottom three plots show how the average density of the dense fuel ball, the total fuel <ρR>, and the dense ball's energy evolve as mass accumulates in the dense ball. This capsule absorbs 150 kJ from a peak x-ray drive temperature of 250 eV. ; v_{imp}~1.95e7 cm s^{-1}, IFAR~36, r_{ball}~ 400-500 g cm^{-3}. The density peaks before <ρR> and well before most of the fuel has accumulated in the ball.

Fig. 14 is for our NIF-scale capsule but with low initial T as just above. The top three plots are of DT density vs radius r, cumulative volume (r^3), and cumulative total (internal + kinetic) energy, all at the time of peak <ρR>. It is immediately apparent that at this time, the volume fraction of the central hot plasma is very small, that the dense fuel occupies about 1/4 of the total fuel volume, and that about 60% of the fuel energy resides in dense fuel. At all times during the stagnation phase there is a reasonably well-defined outer boundary to the dense fuel, and we shall call everything within that boundary the dense "ball". The bottom three plots in Fig. 14 show how the stagnation proceeds with time as more and more of the fuel is accumulated within the ball. We plot the average density of the ball, the total (ball and less compressed fuel) DT <ρR>, and the fuel energy accumulated within the ball, as functions of the fraction of the fuel mass that has been accumulated within the ball. In an ideally efficient world, the ball density, and the <ρR> would peak when the fuel mass and energy had finally all accumulated in the dense ball. Here we see that insofar as <ρR> is concerned we can probably afford to wait for all the fuel to accumulate (2.1 g cm^{-2} *vs* peak of 2.5 g cm^{-2}), but if we do, the fuel ball density will

have fallen to 60% of its peak value, increasing the ignition energy cost ($\propto\rho^{-2}$) by almost a factor of 3.

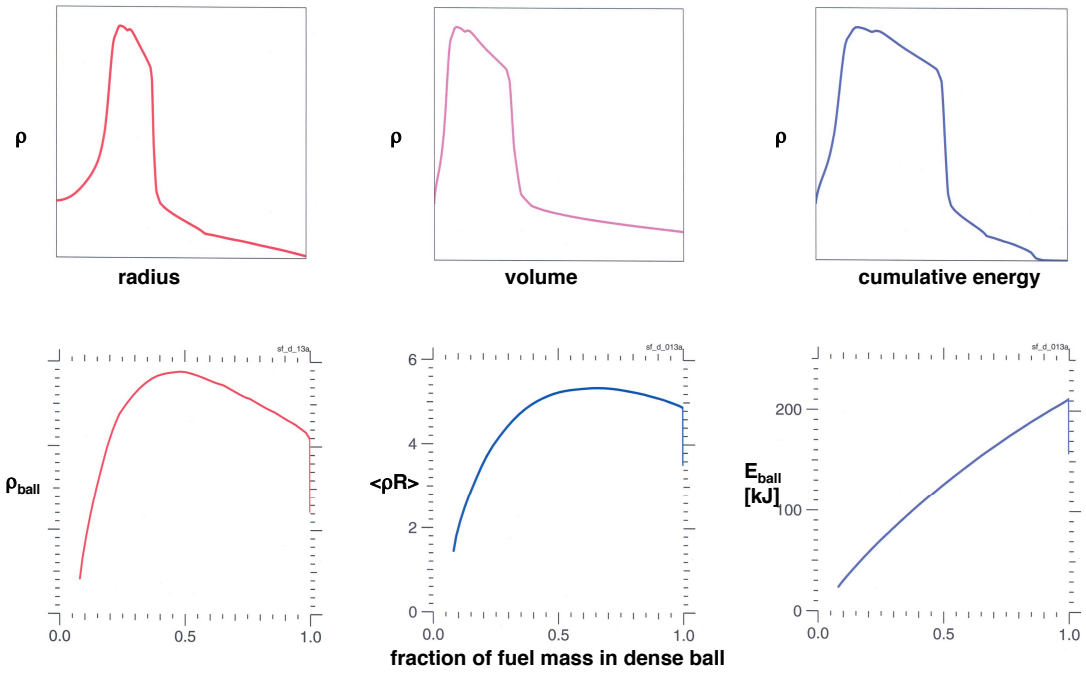

Fig. 15. Central gas and thick fuel effects in a 1-D simulation of the implosion of a capsule with higher initial aspect ratio, lower fuel to ablator mass ratio, and higher implosion velocity than the baseline capsule. The implosion has v_{imp}~2.5e7 cm/s, IFAR~60, r_{ball}~ 450-550 g/cc. Here ball density peaks near peak <ρR> and falls only about 25% before all of the fuel accumulates into the ball. (This was calculated as an IFE-scale capsule so the fuel total energy is much higher and the accumulation time is about 800 ps.)

Fig. 15 shows a similar analysis for a different, higher initial aspect ratio capsule, with a smaller ratio of fuel to ablator mass and hence higher implosion velocity in spite of lower drive temperature (213 *vs* 250 eV). This capsule implodes with a higher inflight aspect ratio (IFAR=shell-radius/shell-thickness when the shell is at 3/4 of its initial radius) and hence is more vulnerable to breakup. Tabak[1] suggests that FI capsules with gains of 100-200 will have IFAR~100, but that most adequately stable implosions for CHS ignition have IFAR<40.) There is still gas in the center, but the cavity is only about 10% of volume at peak <ρR>, and it has consumed only about 10% of the fuel energy for its compression. In this case, however, the ball density peaks later in the fuel accumulation, at the 50% point, and falls less before all of the fuel has accumulated so that it will take only about 70% more energy to ignite the entire fuel mass compared to the ball at peak density. Implosion design to efficiently stagnate the fuel into a uniform, dense ball is a wide open arena for research, having received only a tiny fraction of the effort that has gone into implosions for CHS ignition.

It may be possible to do very well indeed if one can tailor the implosion well enough. Clark and Tabak[29] have verified with 1-D radiative-hydro simulations, using the HYDRA[30] code, that a limit of one of the analytic, self-similar implosion models of Guderley[31] and of Meyer-ter-Vehn and Schalk[32] gives the sort of uniform compression desired — effectively without compressing a central hot plasma and with the ball density increasing as the ball mass increases. Figure 16 illustrates how the analytic and simulated implosions evolve. Driving the implosion that prepares the detailed initial conditions for such a stagnation — that is the run of density, velocity, and pressure — would seem to be the main challenge, but investigations have only begun in this area.

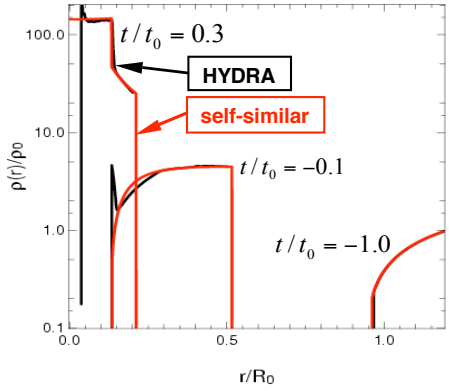

Fig. 16. Full 1-D, radiative-hydrodynamic simulation and analytic calculation of a self-similar implosion designed to produce a uniform dense fuel ball at stagnation.

V. Conclusions

We have discussed above the history and advantages of the cone-guided implosion concept for FI. Investigations via simulation and experiment have begun and shown considerable promise, but the hydrodynamics has not received nearly as much attention as it has for conventional hot-spot ignition. There is a very large parameter space to be investigated for optimizing this concept. A relatively modest simulation scheme has proved adequate, *vis a vis* experiment, for calculating much of the implosion hydrodynamics and for investigating various optimizations. Experiments have verified the promise of the concept — it works. Backlit and self-emission x-radiography can and has revealed many important details, for optimization, about the implosion, such as pre-heat effects, mixing, jet production and impacts, relative timing of events, and actual compression achieved.

The central gas can be partially eliminated by a narrow cone implosion, but the vacuum near the cone tip may collapse. Alternatively, an asymmetrically driven implosion can remove the central gas by jetting it away, but the result is a rather poor conversion of implosion kinetic energy into compression of the fuel. The burn-up fraction of a dense core can be greatly enhanced in fast ignition if the initial ignition wraps around more dense fuel as this can drive addition convergence and very robust burning of the central fuel. Imploded configurations with $<\rho R>$ less than about 1.5 g cm^{-2}, when fast-ignited, do not seem to achieve adequate burn-up fractions.

For this concept to realize its full promise, 1-D implosion design of the capsules needs development. Since a central hot spot is not required or desirable, the implosion should end with

a very small fraction of fuel volume and energy in a high entropy plasma, whether it resides at the center of the dense core or will be jetted away in the full 2-D implosion. Unlike CHS ignition, the goal is an implosion that efficiently results in a near uniform ball, or egg, of high density fuel. How to do this is a rather new area to ICF and has just begun to be explored. Thicker fuel layers are allowed for fast ignition, but to exploit them will require different capsule design strategies from CHS ignition capsules in order to achieve maximum imploded fuel density when almost all of the fuel mass has stagnated.

Acknowledgements

This work was performed under the auspices of the U.S. Department of Energy by the University of California, Lawrence Livermore National Laboratory under Contract No. W-7405-Eng-48.

Figure Captions

Fig. 1. Schematic for an indirectly driven, cone-guided implosion. A re-entrant tube and cone provide a vacuum path for the ignitor beam to near the imploded, high density core. The direct-drive scheme is very similar except the main laser beams shine directly on the capsule, and there is no hohlraum.

Fig. 2. 2-D Lagrangian calculation scheme and some of the design parameters to be optimized.

Fig.3. Baseline design for indirectly driven, NIF scale, cone-guided FI target. The capsule absorbs about 150 kJ of x-rays and the imploded configuration has a solid-angle-averaged fuel column density, $\langle \rho R \rangle_{DT} = 2.18$ g cm^{-2}.

Fig. 4. X-ray drive (a) and direct laser drive (b) targets used to test the hydrodynamics of cone-guided implosions on Omega. Dimensions are shown by the 1mm scale.

Fig. 5. Back-lit x-radiograph images of x-ray drive targets at stagnation with a) linear and b) log gray scale, and c) simulation using linear gray scale. The experiment, unlike the simulation, shows a thread of opaque material leaking from the cone into a dense shell center. In b) the thin colored line shows the original shape of the cone, the thick white line shows the border of the completely opaque region. All the images are to the same scale.

Fig. 6. Simulated and experimental backlit x-radiographs of directly-driven Omega targets. These experimental radiographs (using a Vanadium, ~5 keV backlighter) show a strong cone-shell interaction at late times, and perhaps more convergence than predicted.

Fig. 7: Back-lit x-radiograph images of direct drive targets at stagnation a) with Fe filter to (largely) eliminate self-emission, and b) with same filter and off-center collapse. Each contained ~ 5 atm D_2. Cone and core centerlines are drawn as guides to show the ~25 μm offset in b). c) Lineouts across the images in a) (red) and b) (blue) showing that the offset limited the compression (FWHM increased from 80 to 120 μm), and reduced core gas self-emission (the apparent absorbed fraction increased from 0.65 to 0.75).

Fig. 8. a) The actual tip height was calculated by fitting the shadow of the ledge to an ellipse whose orientation and size was held fixed for all images in a sequence and assumed to be centered under the tip. b) Calculated tip height vs time for filled(triangles) and capsules (squares and Xs), and from LASNEX simulation of a gas filled capsule (smooth line). The LASNEX curve shows the "observed" tip collapse. The simulation shows the initial collapse starting ~ 0.2 ns earlier but being hidden from view by the region around it (as in Fig. 5b).

Fig. 9. MIXS self-emission images complement the backlit Omega capsule implosion images. The time sequence clearly shows emission from the jet impacting the cone and then emission from core stagnation.

Fig. 10. Variations on the NIF-scale baseline design a). Narrower cone, b) produces a less hollow core and higher $<\rho R>$, but jet pinches cone so that cone vacuum is 30% further away. Asymmetric drive, c), which has 10% P_1 in flux, in the sense shown, produces a very compact core that is closer to cone vacuum, but the jet has strongly impacted the cone tip, and the red density contour contains only about 10% of the original fuel mass.

Fig. 11. The *shape* of dense core and of the ignitor deposition can generate additional convergence which generates a very robust ignition and a higher fuel $<\rho R>$ for higher burn-up fraction and higher yield.

Fig. 12. Omega-scale direct drive implosion simulations showing peak $<\rho R>$ configurations to demonstrate the effects of implosions along cones with gaps at the cone tip. Simulation D shows the result for a hemi-spherical capsule (180° "cone"). In all three simulations with holes the plasma jet from the capsule put the critical density for 1μm laser light at about 200μm from the dense core.

Fig. 13. Density profiles at peak $<\rho R>$ for the baseline, NIF-scale capsule with an initial DT vapor density in the capsule of 3.e-5 g cm^{-3} (blue) and for the same capsule with an initial vapor density of 1.e-6 g cm^{-3} (red). The initial vapor densities correspond to initial cryogenic DT temperatures of about 15°K and 11.5°K respectively.

Fig. 14. Central gas and thick fuel effects in a 1-D simulation of the implosion of the NIF-scale baseline capsule with initial vapor density of 1.e-6 g cm^{-3}. The top three plots are "snapshots" at peak $<\rho R>$ of the runs of density *vs* radius, *vs* cumulative volume (r^3), and *vs* cumulative energy. The bottom three plots show how the average density of the dense fuel ball, the total fuel $<\rho R>$, and the dense ball's energy evolve as mass accumulates in the dense ball. This capsule absorbs 150 kJ from a peak x-ray drive temperature of 250 eV. ; v_{imp}~1.95e7 cm s^{-1}, IFAR~36, r_{ball}~ 400-500 g cm^{-3}. The density peaks before $<\rho R>$ and well before most of the fuel has accumulated in the ball.

Fig. 15. Central gas and thick fuel effects in a 1-D simulation of the implosion of a capsule with higher initial aspect ratio, lower fuel to ablator mass ratio, and higher implosion velocity than the baseline capsule. The implosion has v_{imp}~2.5e7 cm/s, IFAR~60, r_{ball}~ 450-550 g/cc. Here ball density peaks near peak $<\rho R>$ and falls only about 25% before all of the fuel accumulates into the ball. (This was calculated as an IFE-scale capsule so the fuel total energy is much higher and the accumulation time is about 800 ps.)

Fig. 16. Full 1-D, radiative-hydrodynamic simulation and analytic calculation of a self-similar implosion designed to produce a uniform dense fuel ball at stagnation.

References

[1] M. TABAK, "Introduction to Fast Ignition", this volume.

[2] S. ATZENI and J. MEYER-TER-VEHN, *The Physics of Inertial Fusion*, Clarendon Press, Oxford (2004).

[3] M. TABAK et al, Lawrence Livermore National Laboratory, Report No. IL8826B, (1997), unpublished.

[4] R. KODAMA et al, "Fast heating of ultrahigh-density plasma as a step towards laser fusion ignition", *Nature*, **412**, 798 (2001).

[5] L.P. FEOKTISTOV, *Budustchee Nauki (Future of Science)*, **18**, 168, Znanie, Moscow (1985), (in Russian).

[6] M. SHMATOV, *Fus. Sci. Tech*. **43**, 456 (2003)

[7] S. HATCHETT and M. TABAK, "Cone-Focussed Target Design for Fast Ignition", 30th Anomalous Absorption Conf., Ocean City, Maryland (2000).

[8] R. KODAMA et al, "Fast heating scalable to laser fusion ignition", *Nature*, **418**, 933 (2002)

[9] R. KODAMA et al, "Plasma devices to guide and collimate a high density of MeV electrons", *Nature*, **432**, 1005 (2004).

[10] M. KEY et al, "Proton Fast Ignition", this volume.

[11] S. CHANDRASEKHAR, *Hydrodynamic and Hydromagnetic Stability*, Clarendon Press, Oxford (1961).

[12] J. A. HARTE et al, "LASNEX — A 2-D Physics Code for Modelling ICF", Lawrence Livermore National Laboratory, Livermore, CA, Report No. UCRL-LR-105821-96 (1997). Available online at http://www. llnl.gov/nif/icf/icfpubs/annuals/96-Annual.pdf

[13] J. HAMMER (private communication).

[14] T. R. DITTRICH et al., *Phys. Plasmas*, **5**, 3708 (1998).

[15] R. B. STEPHENS, "Implosion hydrodynamics of fast ignition targets", *Phys. Plasmas*, **12**, 05312 (2005).

[16] T.R. BOEHLY, *Opt. Commun.*, **133**, 495 (1997).

[17] R. B. STEPHENS et al, *Phys. Rev. Lett.*, **91**, 185001 (2003).

[18] C. STOECKL et al, "Fuel assembly experiments with gas-filled cone-in-shell fast-ignitor targets on OMEGA", submitted to *Phys. Rev. Lett.*

[19] A.J. BUREK and B. YAAKOBI, National Technical Information Service Document No. DE83015439 (1983). Available from National Technical Information Service, Springfield, VA 22161.

[20] G.A. BURGINYON et al, *Proc. SPIE*, **1736**, 36 (1992).

[21] P. AMENDT, R.E. TURNER, and O.L. LANDEN, *Phys. Rev. Lett.*, **89**, 165001 (2002).

[22] H. SHIRAGA et al., *Rev. Sci. Instr*. **68,** 745 (1997).

[23] R. KODAMA et al, "Fast plasma heating in a cone-attached geometry - toward fusion ignition", *Nuclear Fusion*, 44, S276-283 (2004).

[24] M.C. HERRMANN, S.P. HATCHETT, and M.TABAK, "Reducing Ignitor Energy for Fast Ignition by Controlling Energy Deposition", *Bul. Am. Phys. Soc.*, **46**, 106 (2001).

[25] J.D. LINDL, *Inertial Confinement Fusion,* Springer-Verlag, New York (1998).

[26] D.L. HANSON et al, "Z-Pinch-Driven Hemispherical Capsule Implosions for Fast Ignitor Fuel Assembly", American Physical Society, 46th Annual Meeting of the Division of Plasma Physics, 15-19 November, 2004, Savannah, GA. MEETING ID: DPP04., abstract #CP1.096

[27] T.A. MEHLHORN et al, "Recent experimental results on ICF target implosions by Z-pinch radiation sources and their relevance to ICF ignition studies", *Plasma Phys. Control. Fusion*, **45**, A325 (2003).

[28] P.C. Souers, *Hydrogen Properties for Fusion Energy*, Univ. of California Press, Berkeley (1986).

[29] D. CLARK and M. TABAK, "Self-similar implosions for fast ignition", *Bull. Am. Phys. Soc.*(submitted). 47th Annual Mtg of Div. of Plasma Phys., Am. Phys. Soc., Denver, Colorado (2005); M. TABAK et al, "Review of Progress in Fast Ignition", *Phys. Plasmas*, **12**, 057305 (2005).

[30] M.M. MARINAK et al, *Phys. Plasmas*, **8**, 2275 (2001).

[31] G. GUDERLEY, *Luftfahrtforschung*, **19**, 302 (1942).

[32] J. MEYER-TER-VEHN and C. SCHALK, *Z. Naturforsch.*, **37a**, 955 (1982). See also the discussion of similarity solutions in Ref 2.